Experimental Studies on the Performance of a PCM Based Thermal Storage Unit Embedded With Metal Inserts

N. Lakshmi Narasimhan*, Ashwin S, Ajai Rao R, Agni A.S, Harish Kumar S
Department of Mechanical Engineering, SSN College of Engineering, Kalavakkam, 603110, Tamilnadu, India.
***Corresponding author: E-mail: lakshminaras74@gmail.com**

ABSTRACT

The present work investigates a shell and tube type latent heat thermal storage (LHTS) unit employing a high temperature commercial inorganic PCM - HS 89 embedded with metal inserts. Experiments were conducted for both charging and discharging process of the LHTS unit built for the purpose. The results showed that the presence of metal inserts yielded a nearly uniform temperature distribution within the LHTS unit and enhanced the heat transfer rate during charging as well as discharging. The transverse heat conduction due to metal inserts was found to be higher during charging compared to discharging. Charging the unit for a period of about 5 hours resulted in an energy discharge over a period of 1 hour while maintaining the heat transfer fluid exit temperature between 40 and 55°C for the same flow rate.

KEY WORDS: PCM, metal inserts, energy, energy storage, LHTS.

1. INTRODUCTION

Latent heat thermal storage (LHTS) has gained significant attention in the recent past. Owing to its advantages such as high energy storage density and nearly uniform temperature of operation, LHTS systems have been successfully employed in a wide range of applications such as automotives, HVAC, solar thermal, building cooling, electronic cooling, textiles and so on for thermal storage and management. LHTS systems employ phase change materials (PCMs) for the storage/retrieval of thermal energy. PCMs are chemical substances that undergo repeated melting/freezing capable of absorbing/releasing its latent heat of fusion to effect in the energy storage/retrieval process. A detailed review on PCMs and its applications has been presented elsewhere (Farid, 2004; Sharma, 2009).

The main drawback of PCMs is their poor thermal conductivity that results in poor energy charging/discharging characteristics of LHTS units. Several methods such as improving the thermal conductivity of PCMs (Siegel, 1977; Seeniraj, 2002; Liwu and Khodadadi, 2011), addition of fins (Seeniraj, 2002), employing multiple PCMs (Seeniraj and Lakshmi Narasimhan, 2008) and dispersion of nano-particles to PCMs (Kumaresan, 2013) have been proposed to improve the thermal performance of LHTS units. Whereas the addition of metallic particles or nano-particles affect the density and thermo physical properties of PCMs, the addition of fins appears to be a relatively simple and straight forward approach for performance enhancement with no compromise on either the density or the properties of PCMs. Though numerous performance enhancement studies on LHTS units are available in the open literature, studies involving commercial inorganic salts are scarce. The aim of this paper is to study the performance of a shell and tube type LHTS unit employing a commercial inorganic PCM – HS89 embedded with thin metal inserts. A test set up was built for the purpose and experiments were conducted for both charging as well as discharging phases, the results of which are discussed.

2. EXPERIMENTAL SETUP

Figure.1, shows the schematic of the experimental setup consisting of a blower-heater assembly integrated to a shell and tube type LHTS heat exchanger. The shell side of the heat exchanger was loaded with about 40±0.5 kg of a commercial inorganic PCM (HS89) procured from Plus polymers, India while the tube side carried the heat transfer fluid (HTF) for transferring heat to/from the PCM. Air was employed as the HTF with a single pass through the tubes. The air flow exiting the heater unit was distributed uniformly to all the tubes by a header provided at the inlet. The exit of air from the heat exchanger was through an exit header provided at the end of the unit. Table.1, gives the geometric specifications of the LHTS unit designed. The total number of tubes employed was 51 arranged in inline pattern with an equal pitch in the longitudinal and transverse directions. The tubes were inserted in thin aluminium metal sheets (inserts) and mounted carefully across the inlet and exit flanges of the heat exchanger. Figure.2, shows the CAD model of the heat exchanger unit with tubes and metal inserts. The PCM was weighed and packed inside the shell after ensuring the shell to be leak proof. Figure.3, shows the LHTS unit while being filled with PCM. The entire assembly before and after the insulation are shown in Figs.4(a) and (b). All the components with exposed metallic surfaces of the heat exchanger and the headers were fully insulated to minimize heat leak to the surroundings. The insulation materials used comprised of three different layers of glass wool, asbestos rope and a sheet of white insulation foam for effective thermal insulation.

The blower employed was a centrifugal type with capacity 365 CFM and 240 W running under 2800 rpm (make EDM Nadi). A 6 kW multi-coiled finned heater with an automatic temperature controller was used for heating the HTF. Temperatures at different locations within the PCM, inlet and exit of the HTF were measured using k-type thermocouples connected to a temperature indicator with an accuracy of ± 0.3°C. The mass flow rate of the HTF (air)

was determined using the measured air velocity exiting the heat exchanger using a vane type anemometer having an accuracy of ± 0.1 m/s. Temperatures were measured every 10 minutes during charging as well as discharging.

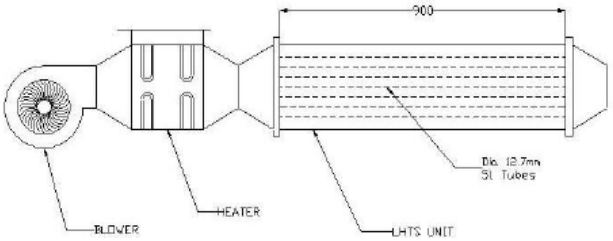

Figure.1. Schematic of the experimental setup

Table.1. Geometrical specifications of experimental setup

Component	Specifications
Air Heater	Duct Dimensions: 165 mm x 210 mm Length of Duct: 600 mm
Shell and Tube Heat Exchanger (Aluminum shell with copper tubes)	Length of tube: 900 mm Diameter of tube: 12.7 mm Shell dimensions: 280 mm x 190 mm Number of tubes: 51 Length of Shell: 900 mm
PCM HS 89	Total Mass used: 40±0.5 kg

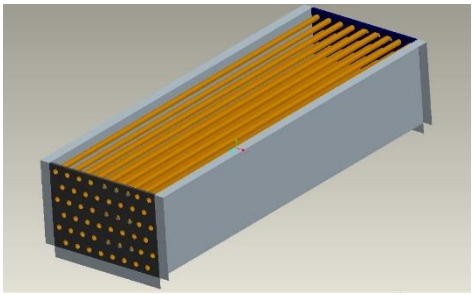

a

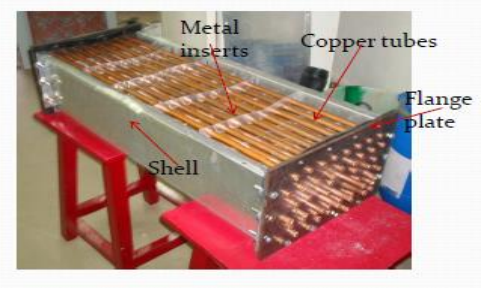

b

Figure.2.(a) CAD model of the heat exchanger unit and (b) pictorial view

Figure.3. Filling the shell with PCM HS89

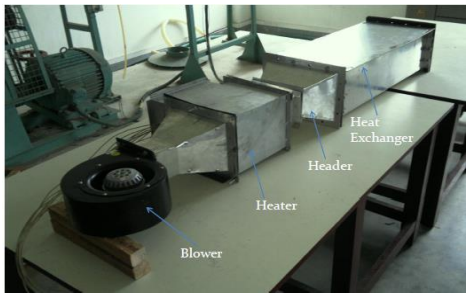

a

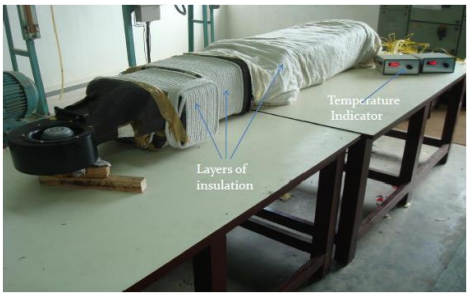

b

Figure.4. Pictorial view of the LHTS unit (a) before insulation and (b) after insulation

Temperatures were measured at 17 different locations within the PCM to investigate the temperature histories during charging and discharging. Figure.5, shows the locations identified using planes of reference at the top, middle and bottom (planes 1, 2 and 3 respectively) for the sake of analysis.

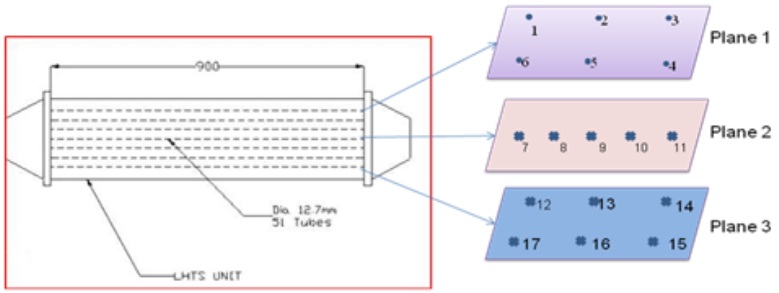

Figure.5. Locations for temperature measurement within the PCM region

3. RESULTS AND DISCUSSION

Experiments were performed on the designed LHTS unit for both charging as well as discharging. The PCM HS89 has a melting point between 87-88^{0}C and latent heat of about 180 kJ/kg specified by the manufacturer. The data on thermal conductivity of the PCM was not available in the manufacturer's technical data sheet. However, simple 1D conduction experiments performed on the PCM beforehand revealed the thermal conductivity to be approximately between 0.45 - 0.5 W/mK. This low thermal conductivity of HS89 emphasizes the need for heat transfer enhancement when using the salt for thermal storage applications. The temperature histories obtained experimentally have been discussed in the following sections.

Charging of PCM:

Variation of HTF Temperature: During charging of the PCM, the HTF (air) temperature was maintained nearly uniform around 120-130^{o}C as shown in Fig.6. While the temperature was oscillating in the first 100 minutes between 112-119^{o}C, later it got stabilized close to 130^{o}C. The reason for the initial drop in the HTF inlet temperature could be attributed to heating up of the side walls of the heater and inlet header after switching on the blower-heater unit. As the temperature of the HTF at inlet was well above the melting temperature of the PCM (88-89^{o}C), it first caused the PCM to get sensibly heated followed by melting and subsequent sensible heating. The HTF transfers heat to the PCM as it flows along the unit. During the first few minutes, the HTF exit temperature was as low as 80^{o}C indicating a larger heat transfer to the PCM owing to a larger HTF-PCM temperature difference. The HTF temperature drop remained as high as 50-60^{o}C between the inlet and exit in the beginning stages while it decreased to about 30-40^{o}C during the later stages of charging of the unit. It can be observed that the HTF exit temperature settled nearly to the melting temperature of the PCM for about 200 minutes during the later stages. This indicates the nearly constant temperature heat addition to the PCM while it underwent the solid-liquid phase change. A higher HTF-PCM fusion temperature difference is required for achieving faster charging of the LHTS unit. However, there is a limit for this temperature difference with inorganic hydrated PCM salts such as HS89 as superheating of the liquid PCM by about 10-15^{o}C may cause gradual disintegration of the water molecules present in the salt. This limit is normally specified by the manufacturers and for the present case it has recommended that the PCM temperature does not exceed 110°C. All measurements at various locations within the PCM ensured that the temperature at no point within the heat exchanger exceeded 110°C during our experiments. On the other hand, a lower HTF-PCM fusion temperature difference would result in a longer duration of charging. A higher HTF-PCM fusion temperature difference is recommended where the availability of the energy source is limited to a shorter duration, while a lower HTF-PCM fusion temperature difference is recommended when the heat source is available for a reasonably longer duration.

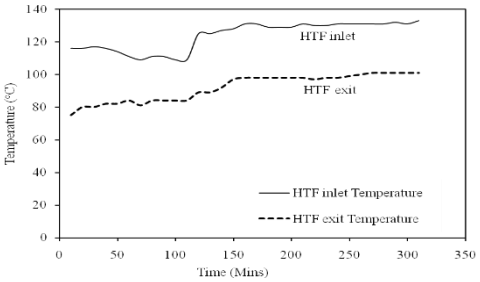

Figure.6. Temporal variation of HTF temperature at inlet and exit during charging

Variation of PCM Temperature: Figures.7-9, shows the time wise variation of PCM temperatures within the unit along the top, middle and bottom planes respectively. The temperatures T1-T6 represent the top plane, T7-T11 represents the mid-plane and T12-T17 represents the bottom plane within the PCM as already discussed (Fig.5). It can be observed from the figures that the PCM temperatures increase gradually and steadily as time progresses. The PCM in and around the mid-plane region is maintained at a higher temperature at all instances of charging compared to the top and bottom planes. The PCM gets sensibly heated until it reaches its fusion temperature of 88°C. It can be observed from Figure.8, that the melting of the PCM occurs first near the inlet section of the heat exchanger as well as in the mid-plane. The PCM essentially remains at a constant temperature of 88°C-89°C during the melting period as observed in Fig.8 for a period of over 125 minutes. Later, the superheating of the liquid PCM occurs in both the

mid-plane region and near to the inlet section of the heat exchanger owing to a relatively higher HTF-PCM temperature difference. Figs.7 and 9, shows that the PCM temperature profiles remain similar in the regions above and below the mid-plane. However, the PCM at the top plane near to the inlet section of the heat exchanger starts melting a little earlier (Fig.7) than that at the bottom plane (Fig.9). It has been observed from the experiments that the PCM far away from the inlet or near the exit of the LHTS unit in both top and bottom planes did not melt even after 5 hours of charging. A still longer charging period was required to ensure complete melting of the PCM within the heat exchanger. The symmetry found between the temperature profiles of the top and bottom planes can be attributed to the presence of metal inserts within the PCM. In the absence of the metal inserts, the thermal resistance within the PCM would be higher owing to its poor thermal conductivity (0.4-0.5W/mK). The addition of metal inserts made of aluminium (k = 170W/mK) improves the overall thermal conductivity and hence the heat transfer within the PCM. Since no data on LHTS units with rectangular cross sections of bigger geometry like the one that is studied presently is available in the open literature, a direct comparison on the performance of the unit without metal inserts in the PCM has not been presented. The symmetry in the temperature profiles noticed in the top and bottom planes indicate the enhanced heat conduction within the PCM along the transverse direction due to the metal inserts.

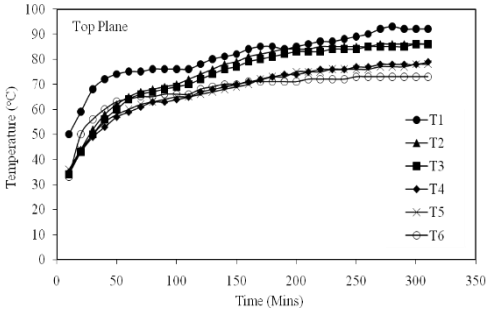

Figure.7. Variation of PCM temperature at top plane (T1-T6) during charging

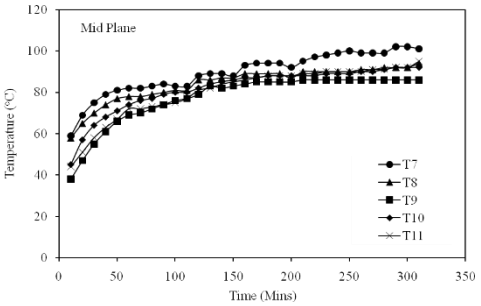

Figure.8. Variation of PCM temperature at middle plane (T7-T11) during charging

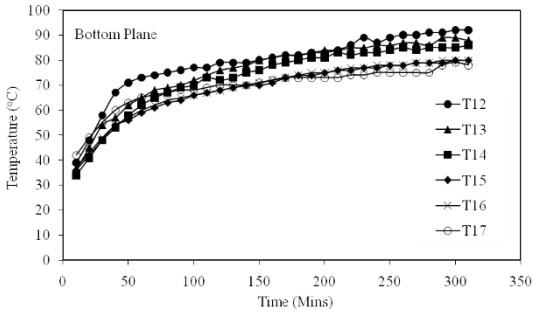

Figure.9. Variation of PCM temperature at bottom plane (T12-T17) during charging

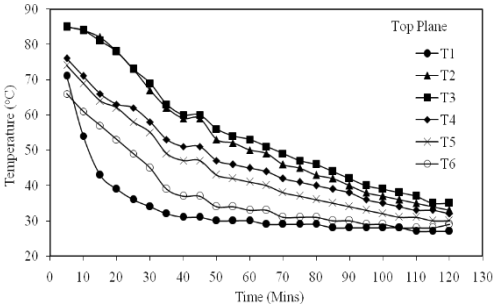

Figure.10. Variation of PCM temperature at top plane (T1-T6) during discharging

Discharging:

Variation of PCM Temperature During Discharging: Similar to the charging experiments, temperature distribution within the PCM along the top, middle and bottom planes at various times have been plotted as shown in Figs.11-13 respectively. It can be seen that the PCM releases the heat to the HTF during discharging until it reaches the ambient temperature. The decrease in PCM temperature at any instant is found to be steep during the first 20 minutes at all locations. The largest slope in the time-temperature curves can be attributed to a high HTF-PCM fusion temperature difference. The slope of the curve reduces as this temperature difference reduces with time. Though the PCM is at its melting temperature (89°C), the steep fall in the PCM temperature is essentially due to enhanced heat transfer rate obtained by the addition of metal inserts to the PCM. In the absence of metal inserts, the fall in temperature could become smaller over a period of time yielding nearly horizontal temperature profiles. The symmetry in the top and bottom planes observed during charging (Figures.7 and 9) could not be observed during the discharging of PCM (Figs.11 and 13). However, the symmetry in the profile was obtained for a short duration of about 30 minutes at regions far away from the entry section in the bottom plane (Fig.12).

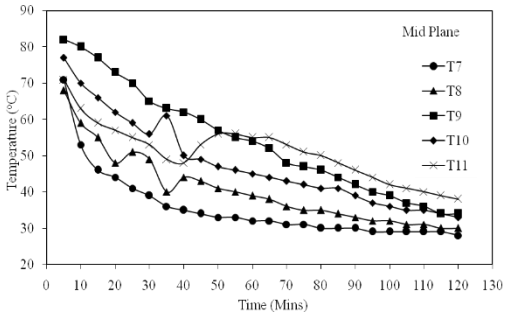

Figure.11. Variation of PCM temperature at middle plane (T7-T11) during discharging

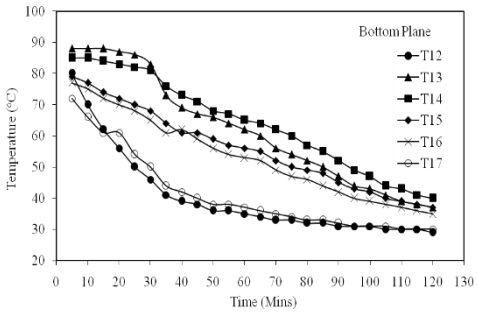

Figure.12. Variation of PCM temperature at bottom plane (T12-T17) during discharging

4. CONCLUSIONS

A shell and tube type LHTS heat exchanger loaded with a commercial inorganic PCM (HS89) embedded with metal inserts has been investigated experimentally. Temperature histories were obtained for both charging as well as discharging of the unit. The use of metal inserts resulted in a nearly uniform temperature distribution within the PCM. The metal inserts improved transverse heat conduction within the PCM more during charging than discharging.

The results showed that with HS89, charging the unit for a period of about 5 hours resulted in an energy discharge for about an hour maintaining the HTF exit temperatures between 40°C and 55°C. The HTF mass flow rates should be relatively lower during discharging compared to that during charging for a better performance and reasonably higher exit temperatures of the HTF.

5. ACKNOWLEDGEMENT

This paper is based on the research work carried under the internal funding scheme of SSNCE. The authors wish to express their sincere thanks to the SSN Trust and SSN College of Engineering for the generous financial support (Ref: IME05/10, Lt. dt 18-06-2010) to carry out the research.

REFERENCES

Farid M.M, Khudhair A.M, Razack S.A.K, Al-Hallaj S, A review on phase change energy storage: materials and applications, Energy Conversion and Management, 45 (9-10), 2004, 31-55.

Kumaresan V, Chandrasekaran P, Maitreyee Nanda, Maini A.K, Velraj R, Role of PCM based nanofluids for energy efficient cool thermal storage system, International Journal of Refrigeration, 36 (6), 2013, 1641-1647.

Liwu Fan, Khodadadi J.M, Thermal conductivity enhancement of phase change materials for thermal energy storage: A review, Renewable and Sustainable Energy Reviews, 15 (1), 2011, 24-46.

Seeniraj R.V, Lakshmi Narasimhan N, Performance Enhancement of a Solar Dynamic LHTS Module having Both Fins and Multiple PCMs, Solar Energy, 82 (6), 2008, 535-542.

Seeniraj R.V, Velraj R, Lakshmi Narasimhan N, Thermal Analysis of a Finned-Tube LHTS module for a Solar Dynamic Power System, Heat and Mass Transfer, 38 (4-5), 2002, 409-417.

Seeniraj R.V, Velraj R, Narasimhan N.L, Heat transfer enhancement study of a LHTS unit containing dispersed high conductivity particles, ASME J. Solar Energy Engineering, 124 (7), 2002, 243-249.

Sharma, Review on thermal energy storage with phase change materials and applications, Renewable and Sustainable Energy Reviews, 13, 2009, 318-345.

Siegel R, Solidification of low conductivity material containing dispersed high conductivity particles, International Journal of Heat and Mass Transfer, 20 (10), 1977, 1087-1089.